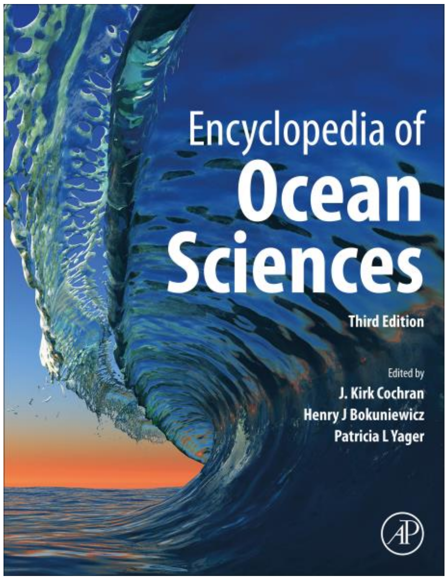

Foltz Gregory R. 2019 Wind- and Buoyancy-Forced Upper Ocean. In Cochran, J. Kirk; Bokuniewicz, J. Henry; Yager, L. Patricia (Eds.) Encyclopedia of Ocean Sciences, 3rd Edition. vol. 1, pp. 113-121, Elsevier. ISBN: 978-0-12-813081-0

dx.doi.org/10.1016/B978-0-12-409548-9.11336-3

Wind- and Buoyancy-Forced Upper Ocean☆

Gregory R Foltz, NOAA Atlantic Oceanographic and Meteorological Laboratory, Miami, FL, United States

Nomenclature

B_0	Surface buoyancy flux
C_D	Drag coefficient
C_E	Latent heat flux transfer coefficient
C_H	Sensible heat flux transfer coefficient
c_p	Specific heat capacity of water
c_{pa}	Specific heat capacity of air
E	Rate of evaporation
g	Acceleration due to gravity
h	Mixed layer depth
L	Latent heat of evaporation
L_{MO}	Monin-Obukhov depth scale
P	Rate of precipitation
q_a	Specific humidity of the air
q_s	Saturated specific humidity at the sea surface temperature
Q_0	Net surface heat flux entering the ocean
Q_{lat}	Latent heat flux due to evaporation
Q_{lw}	Net infrared (longwave) radiation
Q_{sen}	Sensible heat flux
Q_{sw}	Net solar (shortwave) radiation
S_0	Surface salinity
T_a	Air temperature
T_s	Surface ocean temperature
u_a	Air velocity
u_s	Surface ocean velocity
u_*	Oceanic frictional velocity
α	Thermal expansion coefficient
β	Haline contraction coefficient
κ	Von Kármán constant
ρ	Ocean density
ρ_a	Air density
ρ_{fw}	Density of fresh water
τ_0	Wind stress

☆*Change History*: June 2018. GR Foltz updated Abstract, Surface Heat Flux, Wind Forcing, The Seasonal Cycle (all subsections), Further Reading, and Figs. 2, 3, 4, and 5.

This is an update of M.F. Cronin, J. Sprintall, Wind- and Buoyancy-Forced Upper Ocean, *Encyclopedia of Ocean Sciences* (2nd Edn), edited by John H. Steele, Academic Press, 2008, pp. 337–345.

Introduction

Forcing from winds, heating and cooling, and rainfall and evaporation has a profound influence on the distribution of mass, heat, and momentum in the ocean. Although the effects from wind and buoyancy forcing are ultimately felt throughout the entire ocean, the most immediate impact is on the surface mixed layer, where active air-sea exchanges occur. The mixed layer is warmed by the sun and cooled by radiation emitted from the surface and latent heat lost during evaporation (Fig. 1). The mixed layer also tends to be cooled by sensible heat loss since the surface air is generally cooler than the ocean's surface. Evaporation and precipitation change the salinity of the mixed layer. Combined, the salinity and temperature changes define the ocean's surface buoyancy. As the surface loses buoyancy, the surface water can become denser than the water below it, causing convective overturning and mixing. Wind forcing can also cause near-surface overturning and mixing, as well as more localized mixing at the base of the mixed layer through shear-flow instability. This wind- and buoyancy-generated turbulence causes the near-surface water to be well mixed and vertically uniform in temperature, salinity, and density. If the turbulence is strong enough, it can entrain deeper water into the surface mixed layer, causing the surface temperature and salinity to change and the layer of well-mixed, vertically uniform water to thicken. Wind forcing also sets up oceanic currents and can cause changes in the mixed layer temperature and salinity through horizontal and vertical advection.

Although the ocean is forced by the atmosphere, the atmosphere can also respond to ocean surface conditions, particularly sea surface temperature (SST). Direct thermal circulation, in which moist air rises over warm SSTs and descends over cooler SSTs, is prevalent in the tropics. The resulting atmospheric circulation cells influence the patterns of cloudiness, rainfall, and winds that combine to form the wind and buoyancy forcing of the ocean. Thus, the oceans and atmosphere form a coupled system in which it can be difficult to distinguish forcing from response. Because the ocean has a density and heat capacity that are nearly three orders of magnitude greater than the atmosphere, the ocean has larger mechanical and thermal inertia relative to the atmosphere. The ocean therefore acts as memory for the coupled ocean-atmosphere system.

This article begins with a discussion of air-sea interaction through surface heat fluxes, moisture fluxes, and wind forcing. The primary external force driving the ocean-atmosphere system is heating from the sun. Because of the fundamental importance of solar radiation and its seasonal variations, the surface wind and buoyancy forcing are illustrated with two examples of the seasonal

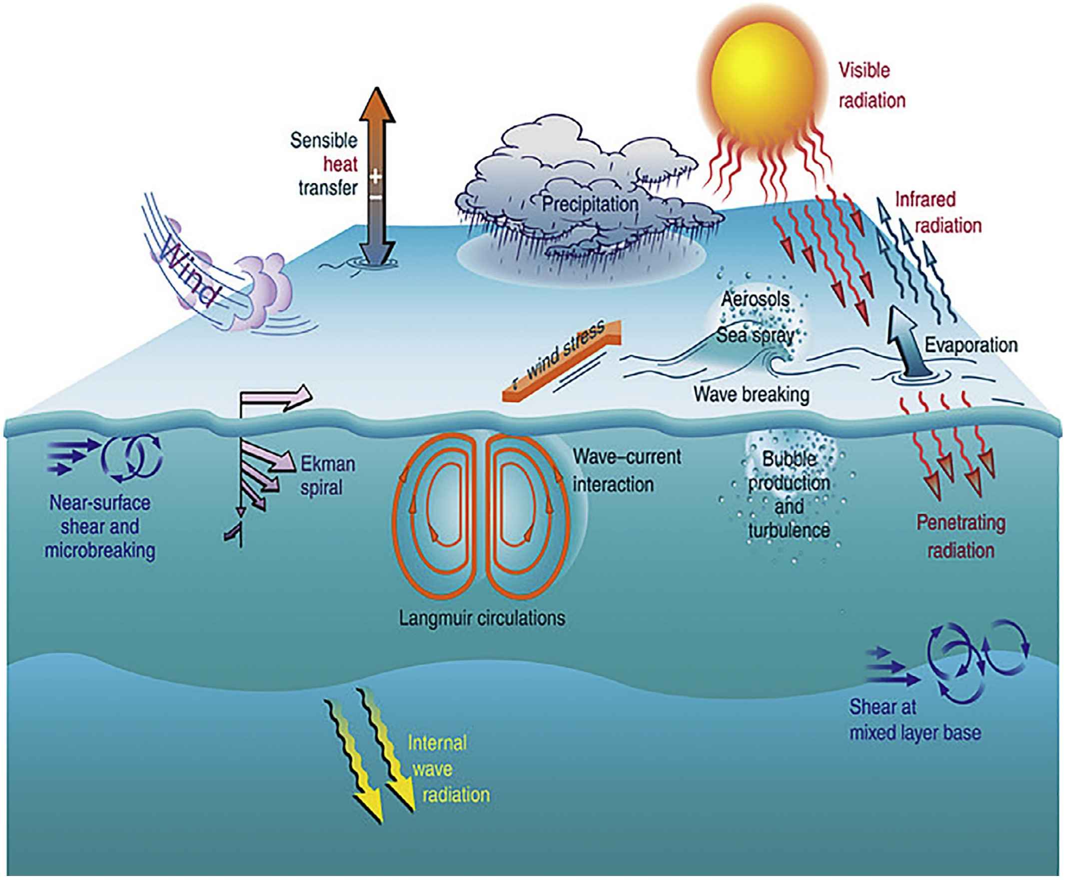

Fig. 1 Schematic drawing of wind- and buoyancy-forced upper ocean processes (Weller and Farmer 1992). Original drawing by Jayne Doucette and Paul Oberlander, Woods Hole Oceanographic Institution.

cycle. The first case describes the seasonal cycle in the South Atlantic, a classic example of a one-dimensional (involving only vertical processes) ocean response to wind and buoyancy forcing. In the second example, the seasonal cycle of the eastern tropical Atlantic is discussed. In this region, the atmosphere and ocean are more strongly coupled, so that wind and buoyancy forcing lead to a sequence of events that make cause and effect difficult to determine. The impacts of wind and buoyancy forcing on the surface mixed layer and deeper ocean are summarized in the conclusion.

Air-Sea Interaction

Surface Heat Flux

The net surface heat flux entering the ocean (Q_0) includes solar (shortwave) radiation (Q_{sw}), net infrared (longwave) radiation (Q_{lw}), latent heat flux due to evaporation (Q_{lat}), and sensible heat flux due to the air and water having different surface temperatures (Q_{sen}):

$$Q_0 = Q_{sw} + Q_{lw} + Q_{lat} + Q_{sen} \tag{1}$$

These fluxes are illustrated in Fig. 1. The earth's seasons are largely defined by the annual cycle in the net surface heat flux that is ultimately driven by the astronomical orientation of the earth relative to the sun. The earth's tilt causes solar radiation to strike the winter hemisphere more obliquely than the summer hemisphere, resulting in less warming of the surface in the winter hemisphere. As Earth orbits the sun, winter shifts to summer and summer back to winter in an annual cycle. The exception is in the tropics, defined as the region between the latitudes of 23.5°S and 23.5°N, where the sun is directly overhead twice each year. Here one might expect the seasonal cycle to be semiannual instead of annual However, as will be discussed later, in some parts of the equatorial oceans, the annual cycle dominates due to coupled ocean–atmosphere–land interactions.

Solar radiation entering Earth's atmosphere is absorbed, scattered, and reflected by water in its liquid and vapor forms. Consequently, the amount of solar radiation that reaches the ocean's surface, Q_{sw}, depends on the amount and type of clouds and, to a lesser extent, the amount of water vapor in the atmosphere, called the specific humidity. Particles suspended in the air, called aerosols, can also reflect, absorb, and scatter incoming solar radiation. Examples include sulfate from the burning of fossil fuels, smoke and soot from biomass burning, and sulfur dioxide from volcanoes. The amount of surface solar radiation absorbed by the ocean depends on its albedo, which is the amount of incident solar radiation that is reflected back to space. Under most conditions, the ocean's albedo is about 6%, meaning that the ocean absorbs 94% of the solar radiation that reaches its surface. The amount of this solar radiation that is absorbed by the ocean mixed layer depends on the transmission properties of light in seawater, including the optical clarity. It can be estimated as the difference between the amount of solar radiation entering the surface and the amount penetrating through the base of the mixed layer.

In addition to reflecting a small portion of incident solar radiation, the ocean and the rest of the earth's surface radiate energy at longer infrared wavelengths, similar to a black body (i.e., proportional to the fourth power of the surface temperature expressed in Kelvin). The atmosphere and clouds also emit infrared radiation, and the portion that is emitted downward and reaches the surface is available to heat the ocean. The net longwave radiation, Q_{lw}, is therefore the combination of the outgoing and incoming infrared radiation. The outgoing portion is larger, leading to a net cooling due to Q_{lw}.

The ocean and atmosphere also exchange heat via conduction, called the sensible heat flux. The sensible heat flux acts to reduce any difference in temperature between the surfaces of the atmosphere and ocean. Thus, when the ocean is warmer than the atmosphere, which is nearly always the case, the sensible heat flux will tend to cool the ocean and warm the atmosphere. A similar relationship holds for water vapor. The air at the surface of the ocean is saturated with water vapor since it is in contact with water, while the air just above the surface typically has a relative humidity less than 100%. As a result, moisture tends to evaporate from the ocean. Because it takes energy to convert liquid water to vapor, during evaporation the ocean loses heat at a rate of

$$Q_{lat} = -L(\rho_{fw}E) \tag{2}$$

where Q_{lat} is the latent heat flux, L is the latent heat of evaporation, ρ_{fw} is the freshwater density, and E is the rate of evaporation. Q_{lat} has units of W m^{-2}, and $(\rho_{fw}E)$ has units of kg s^{-1} m^{-2}. The latent heat flux is nearly always larger than the sensible heat flux due to conduction. When the evaporated moisture condenses in the atmosphere to form clouds, heat is released, affecting the large-scale wind patterns. As an extreme example of air-sea latent heat exchange, a hurricane during its lifetime over the ocean can extract as much as 10,000 nuclear bombs' worth of energy (about 60×10^{16} J) from the ocean through latent heat exchange.

Air-sea heat and moisture transfers occur through turbulent processes and are amplified by strong near-surface winds, which enhance turbulence and increase sea spray, bubble production, and wave breaking. Sensible and latent heat loss thus depend on the speed of the surface wind relative to the ocean's surface, $|\boldsymbol{u_a} - \boldsymbol{u_s}|$. The latent ($Q_{lat}$) and sensible ($Q_{sen}$) heat fluxes can be expressed in terms of "bulk" properties at or near the ocean's surface:

$$Q_{lat} = \rho_a L C_E |\boldsymbol{u_a} - \boldsymbol{u_s}|(q_a - q_s) \tag{3}$$

$$Q_{sen} = \rho_a c_{pa} C_H |\boldsymbol{u_a} - \boldsymbol{u_s}|(T_a - T_s) \tag{4}$$

where ρ_a is the air density, c_{pa} is the specific heat of air, C_E and C_H are the transfer coefficients of latent and sensible heat flux, respectively, q_s is the saturated specific humidity at T_s, the SST, and q_a and T_a are, respectively, the specific humidity and temperature of air a few meters above the air–sea interface. The sign convention used here is that a negative flux tends to cool the ocean. The transfer coefficients, C_E and C_H, depend on the wind speed and stability properties of the atmospheric boundary layer, making estimations of the turbulent heat fluxes, Q_{lat} and Q_{sen}, quite difficult. Most algorithms estimate the turbulent heat fluxes iteratively, using initial estimates of the fluxes to compute the transfer coefficients. The dependence of the turbulent heat fluxes on wind speed and SST causes the system to be coupled since the heat fluxes can change the wind speed and SST.

The climatological net surface heat flux, Q_0, and SST for the entire globe are shown in Fig. 2. Several patterns are evident. (Note that the spatial structure of the climatological latent heat flux can be inferred from the climatological evaporation shown in Fig. 3A). On average, the tropics are heated more than the poles, causing warmer SST in the tropics and cooler at the poles. There are significant zonal asymmetries in the net surface heat flux and SST. The largest ocean heat losses occur over the mid-latitude western boundary currents. In these regions, latent and sensible heat fluxes are enhanced due to strong winds that are cool and dry as they blow off of the continents and over the warmer water carried poleward by the boundary currents. In contrast, the ocean's latent and sensible heat losses are reduced in eastern boundary regions, where marine winds blow over cooler water. Consequently, the ocean gains heat from the atmosphere in eastern boundary regions. These spatial patterns exemplify the rich variability in the ocean-atmosphere system that occurs on a variety of spatial and temporal scales. In particular, seasonal conditions are often quite different from the mean climatology. The seasonal warming and cooling in the South Atlantic and eastern equatorial Atlantic are discussed later.

Thermal and Haline Buoyancy Fluxes

Since the density of seawater depends on temperature and salinity, air–sea heat and moisture fluxes can change the surface density, making the water column more or less buoyant. Specifically, the net surface heat flux (Q_0), rate of evaporation (E), and precipitation (P) can be expressed as a buoyancy flux (B_0):

$$B_0 = \frac{-g\alpha Q_0}{\rho c_p} + g\beta(E - P)S_0 \tag{5}$$

where g is acceleration due to gravity, ρ is ocean density, c_p is the specific heat of water, S_0 is surface salinity, α is the thermal expansion coefficient ($-\rho^{-1}\partial\rho/\partial T$), and β is the haline contraction coefficient ($\rho^{-1}\partial\rho/\partial S$). Q_0 has units of W m^{-2} and E and P have units of m s^{-1}. B_0 has units of m^2 s^{-3} and can be interpreted (when multiplied by density and integrated over a volume) as the buoyant production of turbulent kinetic energy (or destruction of available potential energy). A negative (i.e., downward) buoyancy flux, due to either surface warming or precipitation, tends to make the ocean surface more buoyant and stable. Conversely, a positive buoyancy flux, due to either surface cooling or evaporation, tends to make the ocean surface less buoyant. As the water column loses buoyancy, it can become convectively unstable, with heavy water lying over lighter water. Turbulent kinetic energy, generated by the ensuing convective overturning, can then cause deeper, generally cooler water to be entrained and mixed into the surface mixed layer (Fig. 1). Thus, entrainment mixing typically causes the SST to cool and the mixed layer to deepen. As discussed in the next section, entrainment mixing can also be generated by wind forcing, through stirring of the upper ocean and velocity shear at the base of the mixed layer.

The climatological evaporation and precipitation fields are shown in Fig. 3. Note that in terms of buoyancy, a 20 W m^{-2} heat flux is approximately equivalent to a 5 mm day^{-1} rain rate. As a result, in some regions of the world oceans, the freshwater flux term in (5) dominates the heat flux contribution to the buoyancy flux and hence is a major factor in mixed layer thermodynamics. For example, in the tropics, heavy precipitation can result in a surface-trapped freshwater pool that forms a shallower mixed layer within a deeper, nearly isothermal layer. The difference between the shallower mixed layer of uniform density and the deeper isothermal layer is referred to as a salinity-stratified barrier layer. As the name suggests, a barrier layer can limit the turbulent mixing of heat between the ocean surface and the deeper thermocline since the barrier layer water has nearly the same temperature as the mixed layer.

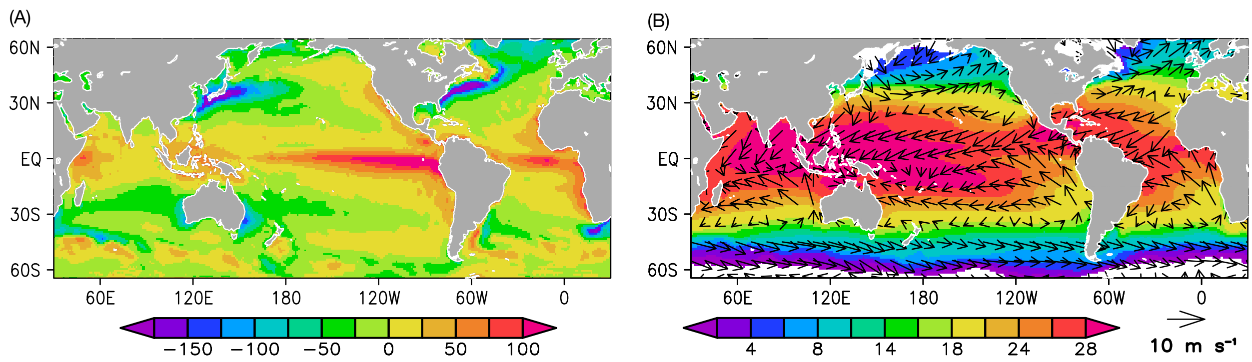

Fig. 2 Mean climatologies of (A) net surface heat flux (W m^{-2}) and (B) SST (°C) and surface winds (m s^{-1}). The scale vector for the winds is shown below (B). Climatologies of heat flux and SST provided by Yu and Weller (2007). Climatology of surface wind is from Kalnay et al. (1996).

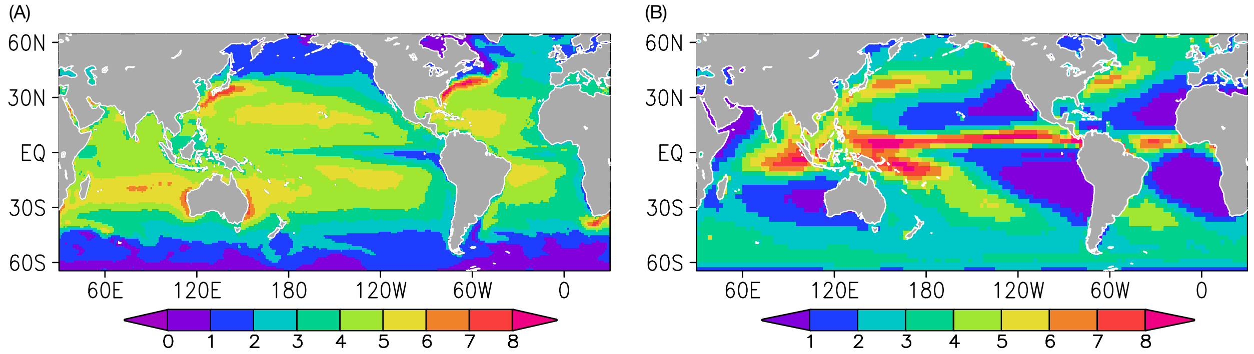

Fig. 3 Mean climatologies of (A) evaporation from Yu and Weller (2007) and (B) precipitation from Adler et al. (2003). Both have units of mm day^{-1}.

Freshwater fluxes can also dominate the surface layer buoyancy profile in subpolar latitudes. During winter, atmospheric cooling of the ocean and stronger wind mixing generates a very deep isothermal layer. Wintertime ice formation then extracts fresh water from the surface layer, leaving a saltier brine that further increases the surface density, decreases the buoyancy, and enhances deep convection. This process can lead to deep-water formation as the cold and salty dense water sinks and spreads horizontally, forcing the deep, slow thermohaline circulation. Conversely, in summer when the ice shelf and icebergs melt, fresh water is released. This causes the density of the surface layer to decrease, and the resultant stable halocline (salinity-induced pycnocline) inhibits the sinking of water.

Wind Forcing

Winds have a strong influence on the ocean's circulation and mass field. Wind blowing over the ocean surface causes a tangential stress ("wind stress") at the interface that acts as a vertical flux of horizontal momentum. Similar to the air-sea fluxes of heat and moisture, the air-sea flux of horizontal momentum, $\boldsymbol{\tau}_0$, can be expressed in terms of bulk properties as

$$\boldsymbol{\tau}_0 = \rho_a C_D |\boldsymbol{u}_a - \boldsymbol{u}_s| (\boldsymbol{u}_a - \boldsymbol{u}_s) \quad (6)$$

where ρ_a is the air density and C_D is the drag coefficient. The drag coefficient determines the sensitivity of $\boldsymbol{\tau}_0$ to changes in the bulk wind speed. Over the ocean, C_D generally becomes larger as wind speed increases, due to an increase in surface wave amplitude and roughness. However, at a wind speed of approximately 40 m s^{-1} (90 mph), C_D levels off and may even decrease with further increases in wind speed. This is thought be caused by extensive wave breaking, sea foam, and sea spray as winds increase beyond a certain threshold. This reduces the surface roughness and the sensitivity of the turbulent transfer of wind momentum to an increase in wind speed, thus reducing C_D. This has important implications for modeling tropical cyclones and predicting their intensities.

The direction of the stress is determined by the orientation of the surface wind, $\boldsymbol{u}_a$, relative to the ocean surface flow, $\boldsymbol{u}_s$. The units of the surface wind stress are N m^{-2}. Wind stress can also be expressed in terms of an oceanic frictional velocity, $\boldsymbol{u}_*$ (i.e., $\tau_0 = \rho \boldsymbol{u}_*^2$). This frictional velocity represents the vertical turbulent flux of oceanic momentum induced by the wind. The frictional velocity is related to the wind-generated oceanic velocity shear, $\partial \boldsymbol{u}/\partial z$, through the nondimensional "von Kármán constant," κ: $\partial \boldsymbol{u}/\partial z = \boldsymbol{u}_*/(\kappa z)$, where z is depth in the ocean. The shear production of turbulent kinetic energy by the wind can therefore be expressed as: $\rho(\kappa z)^{-1} u_*^3 = \tau_0 \partial u/\partial z$, where here u_* and u are the projections onto the direction of the wind stress. Thus, if the wind stress is in the same direction as the oceanic velocity shear, turbulent kinetic energy increases, while wind stress that is in the opposite direction of velocity shear reduces wind-induced turbulent kinetic energy.

The mechanisms by which the momentum flux extends below the air–sea interface are not well understood. Some of the wind stress generates ocean surface waves. However, most of the wave momentum later becomes available to generate currents through wave breaking, and through wave–wave and wave–current interactions. For example, wave–current interactions associated with Langmuir circulation can set up large coherent vortices that carry momentum down to near the base of the mixed layer. Also, as with convective overturning, direct wind stirring can entrain cooler thermocline water into the mixed layer, producing a colder and deeper mixed layer. Likewise, current shear at the base of the mixed layer can cause "Kelvin-Helmholz" instability that further mixes properties within and at the base of the mixed layer.

Variability in the depth of the mixed layer can be understood through consideration of the turbulent kinetic energy (TKE) budget. For example, for a stable buoyancy flux (i.e., "forced convection"), the depth, L_{MO}, at which there is just sufficient mechanical energy from the wind to mix the input of buoyancy uniformly can be found by equating the wind-induced production of TKE, $\rho u_*^3/(\kappa z)$, to the surface buoyancy flux, ρB_0. Here u_* is taken to be the magnitude of the friction velocity. This depth is referred to as the Monin-Obukhov depth scale:

$$L_{MO} = \frac{u_*^3}{\kappa B_0} \quad (7)$$

At depths below L_{MO}, buoyant suppression of turbulence (due to an increase in seawater density with depth) exceeds the mechanical production and there tends to be little surface-generated turbulence. Typically, however, other terms in the TKE budget cannot be ignored. In particular, for an unstable buoyancy flux (i.e., "free convection"), the production of potential energy through entrainment becomes important. Thus, the mixed layer depth is rarely equivalent to the Monin-Obukhov depth scale.

Over timescales longer than roughly a day, the earth's spinning tends to cause a rotation of the vertical flux of momentum. From the noninertial perspective of an observer on the rotating earth, this tendency to rotate appears as a force, referred to as the Coriolis force. When the wind ceases, inertial motion continues and accounts for significant fraction of the total kinetic energy in the global ocean. Vertical shear in the currents, including those associated with inertial oscillations, can cause Kelvin-Helmholz instability and can be a significant source of TKE. The vertical mixing induced by inertial oscillations acts to cool SST and hence affects the coupled ocean-atmosphere system.

For sustained winds beyond the inertial timescale, Coriolis turning causes the wind-forced surface layer transport ("Ekman transport") to be perpendicular to the wind stress. Because the projection of the earth's axis onto the local vertical axis (direction in which gravity acts) changes sign at the equator, the Ekman transport is to the right of the wind stress in the Northern Hemisphere and to the left of the wind stress in the Southern Hemisphere. Convergence and divergence of this transport leads to vertical motion that can lower and raise the thermocline, respectively, thereby generating horizontal pressure gradients that set the subsurface waters in motion. In this way, meridional variations in the prevailing zonal wind stress drive the steady, large-scale ocean gyres.

The influence of Ekman upwelling on SST can be seen along the eastern boundaries of the ocean basins and along the equator (Fig. 2B). Equatorward winds along the eastern boundaries of the Pacific and Atlantic Oceans cause an offshore-directed Ekman transport. Mass conservation requires that this near-surface water be replaced with water upwelled from greater depths, which is generally cooler than the surface waters outside the upwelling zone. Likewise, in the tropics prevailing easterly trade winds cause poleward Ekman transport. At the equator, the poleward transport diverges, leading to upwelling and cooler SSTs (Fig. 2B). The thermal equator (the latitude where SSTs are warmest) favors the Northern Hemisphere in the Atlantic and Pacific Oceans and is generally several degrees north of the equator. The reason is not precisely known, but is likely due to a combination of factors, including the geometry of the continents and the basin-scale meridional heat transports of the ocean and atmosphere.

In the tropics, winds tend to flow from cool SSTs to warm SSTs, where deep atmospheric convection can occur. Thus, the thermal equator is associated with surface wind convergence and rainfall, and this region is referred to as the Intertropical Convergence Zone (ITCZ). The close relationship between the SST gradient and winds accounts for an important coupling mechanism in the tropics.

The Seasonal Cycle

The South Atlantic: One-Dimensional Ocean Response to Wind and Buoyancy Forcing

From 1997 until the present, a surface buoy has been maintained at 10°S, 10°W in the central tropical South Atlantic. The mooring is part of the Prediction and Research Array in the Tropical Atlantic (PIRATA), which consists of 18 moored buoys positioned throughout the tropical Atlantic. The moorings make routine measurements of the near-surface atmosphere and upper ocean. The seasonal climatology at this site (Fig. 4) illustrates a classic near-one-dimensional ocean response to wind and buoyancy forcing. A one-dimensional response implies that only the vertical structure of the ocean is changed by the forcing.

During wintertime (December–February), layers of warmer and lighter water are formed near the surface in response to the increasing solar radiation. Note that the seasonal cycle in the Southern Hemisphere tends to be opposite of that in the Northern Hemisphere, with warmest temperatures and strongest solar radiation generally occurring in Northern Hemisphere winter. By spring, this heating has built a stable (buoyant), shallow seasonal thermocline that traps the warm surface waters. In summer, surface winds increase and net cooling sets in. By fall, the surface layer is mixed by wind stirring and convective overturning. The spring thermocline is eroded and the mixed layer deepens to the top of the permanent thermocline.

To first approximation, horizontal advection does not seem to be important in the seasonal heat budget. The progression appears to be consistent with a surface heat budget described by

$$\frac{\partial T}{\partial t} = \frac{Q_0}{\rho c_p h} \tag{8}$$

where $\partial T/\partial t$ is the local time rate of change of the mixed layer temperature, and h is the mixed layer depth. Since only vertical processes (e.g., turbulent mixing and surface forcing) affect the depth and temperature of the mixed layer, the heat budget can be considered one-dimensional.

A similar one-dimensional progression occurs in response to the diurnal cycle of buoyancy forcing associated with daytime heating and nighttime cooling. Mixed layer depths can vary from just a few meters during daytime to several tens of meters during nighttime. Daytime and nighttime SSTs can sometimes differ by more than 1°C. However, not all regions of the ocean have such an idealized mixed layer seasonal cycle. Our second example shows a more complicated seasonal cycle in which the tropical atmosphere and ocean are coupled.

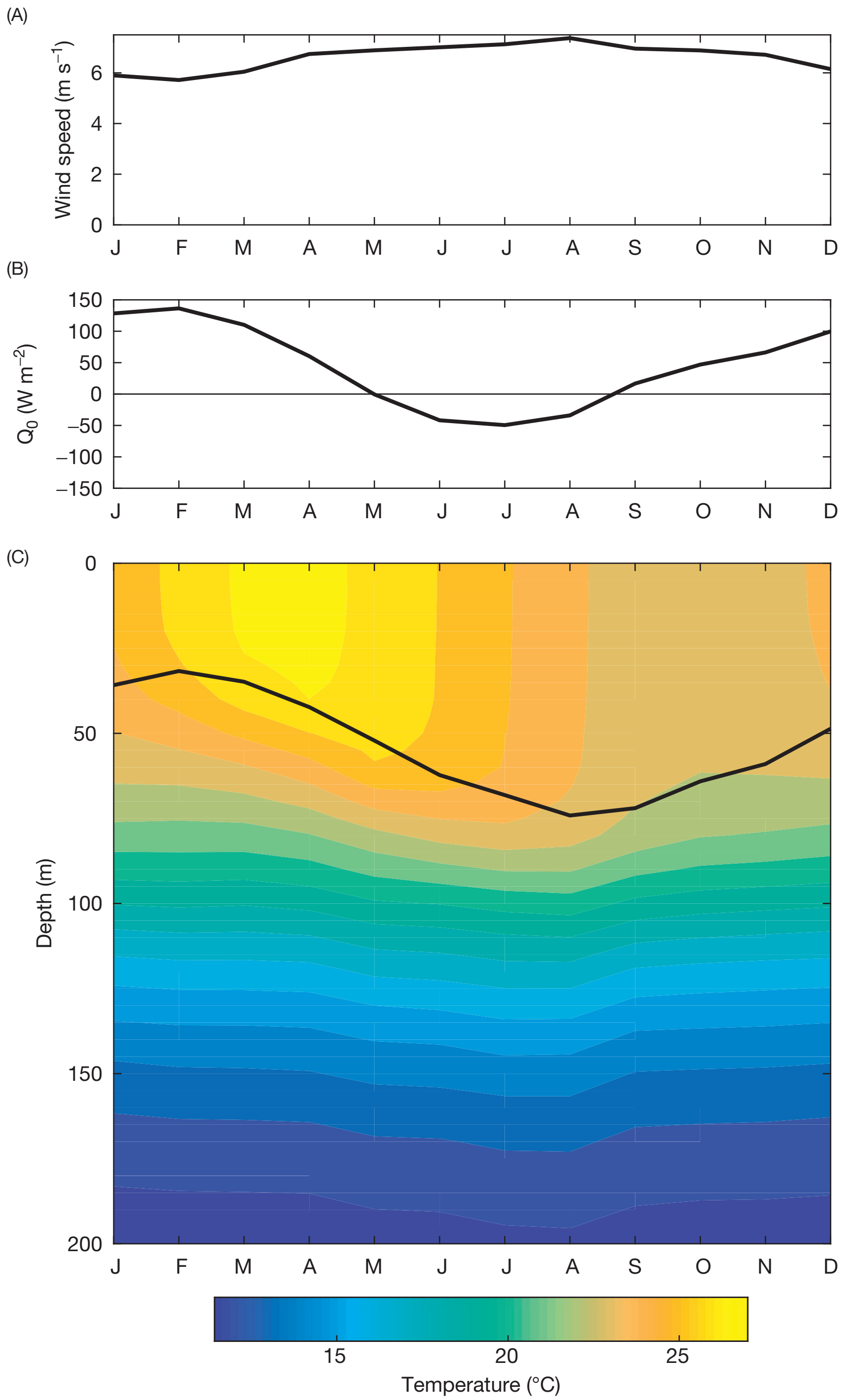

Fig. 4 Seasonal climatologies at the 10°S, 10°W PIRATA mooring in the South Atlantic: (A) Wind speed, (B) net surface heat flux, and (C) upper ocean temperature. The *black line* in (C) represents the base of the mixed layer, defined as the depth where temperature is 0.3°C cooler than the surface temperature.

The Equatorial Atlantic: Coupled Ocean–Atmosphere Variability

Because there is no Coriolis turning at the equator, water and air flow are particularly susceptible to horizontal convergence and divergence. Small changes in the wind patterns can cause large variations in oceanic upwelling, resulting in significant changes in SST and consequently in the atmospheric heating patterns. This ocean and atmosphere coupling thus causes initial changes to the system that perpetuate further changes.

At the equator, the sun is overhead twice per year: in March and again in September. Therefore, one might expect a semiannual cycle in the mixed layer properties. Although this is indeed found in some parts of the equatorial oceans (e.g., in the western Pacific

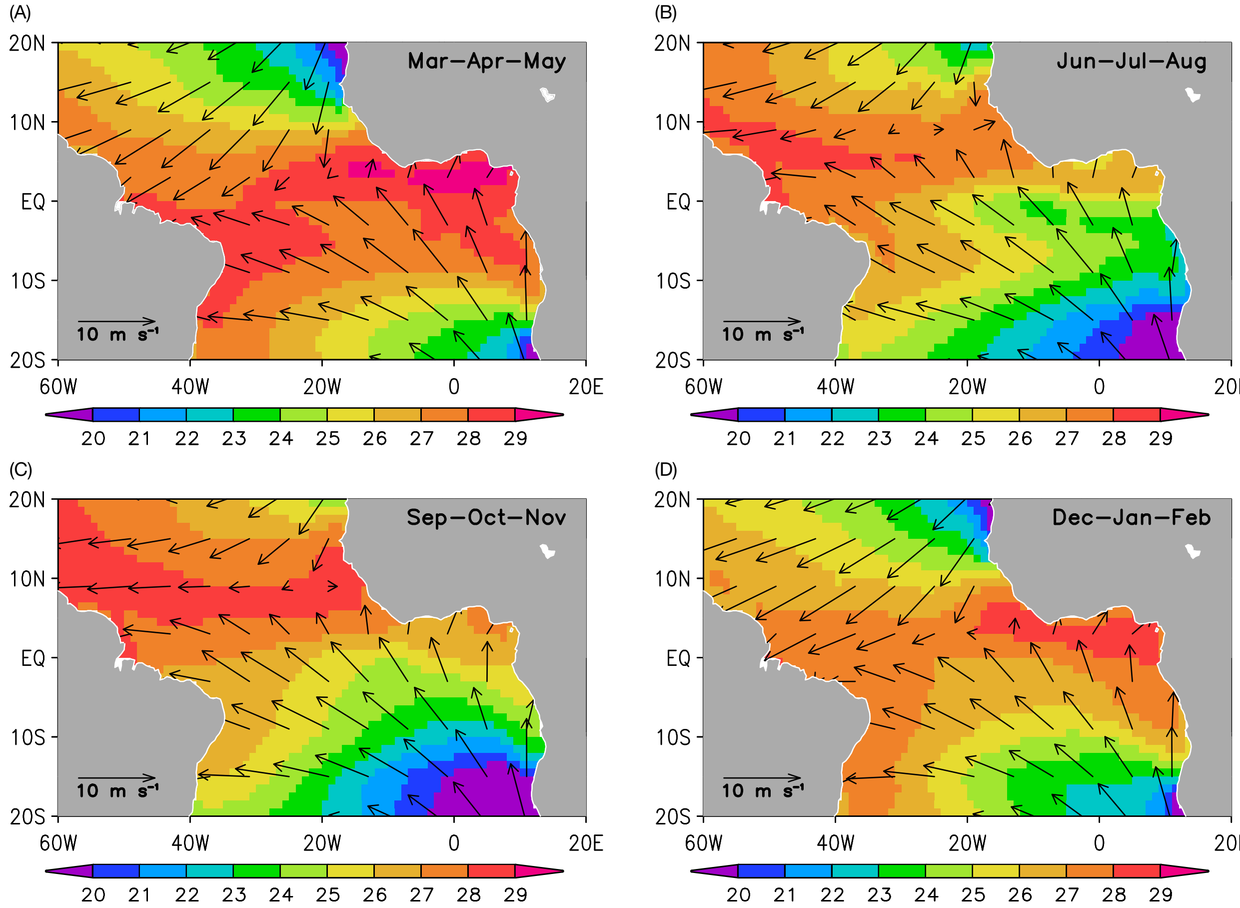

Fig. 5 Seasonal climatologies of the tropical Atlantic SST (°C) and wind (m s^{-1}): (A) Mar.–Apr.–May; (B) Jun.–Jul.–Aug.; (C) Sep.–Oct.–Nov.; and (D) Dec.–Jan.–Feb. Climatologies for SST are from Yu and Weller (2007) and for wind are Kalnay et al. (1996).

and Atlantic), in the eastern equatorial Pacific and Atlantic the annual cycle dominates. During the warm season in the Atlantic (March–May), the solar equinox causes a maximum in insolation, equatorial SST is warm, and the meridional SST gradient is weak (Fig. 5A). Consequently, the ITCZ is near the equator. The weak winds associated with the ITCZ cause a reduction in latent heat loss, wind stirring, and upwelling, all of which lead to further warming of the equatorial SSTs. Thus the warm SST and surface heating are mutually reinforcing.

Beginning in about April–May, SSTs begin to cool in the eastern equatorial Atlantic, perhaps in response to southerly winds associated with the continental monsoon. The cooler SSTs on the equator cause an increased meridional SST gradient that intensifies the southerly winds and the SST cooling in the eastern Atlantic. As the meridional SST gradient increases, the ITCZ begins to migrate northward. Likewise, the cool SST anomaly in the far east sets up a zonal SST gradient along the equator that intensifies the zonal trade winds to the west of the cool anomaly. These enhanced trade winds then produce SST cooling (through increased upwelling, wind stirring, and latent heat loss) that spreads westward (Fig. 5).

During July–August, the equatorial cold tongue is fully formed (Fig. 5B). Stratus clouds, which tend to form over very cool SSTs in the tropical Atlantic, cause a reduction in solar radiation, acting to reinforce the cool SSTs. The large meridional gradient in SST between the equatorial cold tongue and warmer SSTs induced by strong solar heating to the north causes the ITCZ to be at its northernmost latitude during August–October. After the cold tongue is fully formed, the reduced zonal SST gradient within the cold tongue causes the trade winds to weaken there, leading to reduced SST cooling along the equator. Finally, by January–March, the increased solar radiation along and south of the equator, and the reduced heating in the Northern Hemisphere, cause the ITCZ to move back to the equator. With weaker winds, the equatorial SST continues to warm, bringing the coupled system back to the warm season conditions.

Conclusion

Because the ocean mixed layer responds so rapidly to surface-generated turbulence through wind- and buoyancy-forced processes, the surface mixed layer can often be modeled successfully using one-dimensional (vertical processes only) physics. Surface heating and cooling cause the ocean surface to warm and cool; evaporation and precipitation cause the ocean surface to become saltier and fresher. Stabilizing buoyancy forcing, whether from net surface heating or precipitation, stratifies the surface and isolates it from the deeper waters, whereas wind stirring and destabilizing buoyancy forcing generate surface turbulence that causes the surface properties to mix with deeper water. Eventually, however, one-dimensional models drift away from observations, particularly in regions with strong ocean-atmosphere coupling and oceanic current structures. The effects of horizontal advection are explicitly not included in one-dimensional models. Likewise, vertical advection depends on horizontal convergences and divergences and therefore is not truly a one-dimensional process. Finally, wind and buoyancy forcing can themselves depend on the horizontal SST patterns, blurring the distinction between forcing and response.

Although the mixed layer is the principle region of wind and buoyancy forcing, ultimately the effects are felt throughout the world's oceans. Both the wind-driven motion below the mixed layer and the thermohaline motion in the relatively quiescent deeper ocean originate through forcing in the surface layer that causes an adjustment in the mass field (i.e., density profile). In addition, buoyancy and wind forcing in the upper ocean define the property characteristics for all of the major water masses found in the world oceans. On a global scale, there is surprisingly little mixing between water masses once they acquire the characteristic properties at their formation regions and are vertically subducted or convected from the active surface layer. As these subducted water masses circulate through the global oceans and later outcrop, they can contain the memory of their origins at the surface through their water mass properties and thus can potentially induce decadal and centennial modes of variability in the ocean–atmosphere climate system.

References

Adler RF, et al. (2003) The Version 2 Global Precipitation Climatology Project (GPCP) monthly precipitation analysis (1979-present). *Journal of Hydrometeorology* 4: 1147–1167.
Kalnay E, et al. (1996) The NCEP/NCAR 40-year reanalysis project. *Bulletin of the American Meteorological Society* 77: 437–471.
Weller RA and Farmer DM (1992) Dynamics of the ocean mixed layer. *Oceanus* 35: 46–55.
Yu L and Weller RA (2007) Objectively analyzed air-sea heat fluxes for the global ice-free oceans (1981–2005). *Bulletin of the American Meteorological Society* 88: 527–539.

Further Reading

Fairall CF, Bradley EF, Hare JE, Grachev AA, and Edson JB (2003) Bulk parameterization of air-sea fluxes: Updates and verification for the COARE algorithm. *Journal of Climate* 16: 571–591.
Kraus EB and Businger JA (1994) *Oxford monographs on geology and geophysics: Atmosphere-ocean interaction*, 2nd edn. New York: Oxford University Press.
Mitchell T and Wallace JM (1992) The annual cycle in equatorial convection and sea surface temperature. *Journal of Climate* 5: 1140–1156.
Niiler PP and Kraus EB (1977) One-dimensional models of the upper ocean. In: Kraus EB (ed.) *Modeling and prediction of the upper layers of the ocean*, pp. 143–172. New York: Pergamon.
Okumura Y and Xie SP (2004) Interaction of the Atlantic equatorial cold tongue and the African monsoon. *Journal of Climate* 17: 3589–3602.
Price JF, Weller RA, and Pinkel R (1986) Diurnal cycling: Observations and models of the upper ocean response to diurnal heating, cooling, and wind mixing. *Journal of Geophysical Research* 91: 8411–8427.